# Reactive high power impulse magnetron sputtering

J. T. Gudmundsson
*University of Michigan Shanghai Jiao Tong University Joint Institute,*
*Shanghai Jiao Tong University, Shanghai, China and*
*Science Institute, University of Iceland, IS-107 Reykjavik, Iceland*

F. Magnus
*Department of Physics and Astronomy, Uppsala University, Box 530, S-751 21 Uppsala, Sweden*

T. K. Tryggvason, S. Shayestehaminzadeh, O. B. Sveinsson, and S. Olafsson
*Science Institute, University of Iceland, Dunhaga 3, IS-107 Reykjavik, Iceland*

The discharge current waveform in a reactive high power impulse magnetron sputtering (HiPIMS) discharge is highly dependent on both the pulse repetition frequency and the discharge voltage. Here we demonstrate this difference in the discharge current-voltage-time waveforms for a reactive $Ar/O_2$ HiPIMS discharge with a titanium target for 400 $\mu$s long pulses. We show that the discharge current waveform varies with both the pulse repetition frequency and gas flow rate and that the current increases with decreasing frequency. This current variation is attributed to an increase in the secondary electron emission yield during the self-sputtering phase of the pulse, as an oxide forms on the target.

## 1. Introduction

High power impulse magnetron sputtering (HiPIMS) is becoming an established ionized physical vapor deposition technique for deposition of high quality films and functional coatings [1, 2]. Pulsing the target to a high power density with short voltage pulses while maintaining a low duty cycle results in a high electron density [3] which provides a high ionization fraction of the sputtered atoms [4] as well as a high dissociation fraction of molecular gases [5]. Due to this, HiPIMS is particularly promising for deposition of compound films by reactive sputtering. Reactive sputtering, where metal targets are sputtered in a reactive gas atmosphere (e.g. $O_2$, $N_2$ etc.) to deposit compound materials, is of utmost importance in various technologies with applications that include transparent conductive oxides, permeation barrier coatings, hard coatings, etc. Reactive HiPIMS has been demonstrated for the deposition of various compound films including $TiO_2$ [6, 7], TiN [8, 9], ZnO [10], $Nb_2O_5$ [11] and $HfO_2$ [12]. The deposited films have lower surface roughness [7, 8], reach high density at lower substrate temperatures [8] and have lower electrical resistance [9] when grown by HiPIMS compared to dc magnetron sputtering at the same average power.

The presence of a reactive gas can lead to a formation of a compound film on the target and thus there is a change in the target condition [13]. Due to this target coverage, the reactive sputtering process is inherently unstable, and is commonly represented in a familiar hysteresis curve that shows e.g. the deposition rate or the target voltage versus the flow rate of the reactant molecular gas [14]. Sputtering at low reactive gas flows, where there is no significant reaction with the sputtering target, is referred to as metal mode sputtering. For high flows of reactive gas, when a compound has formed on the target, it is referred to as compound mode or poisoned mode sputtering. The hysteresis occurs if the effective etch rate of the compound is lower than for the pure metal, which is commonly the case due to a lower sputter yield of the compound. Also, due to a change in the secondary electron emission yield as a compound is formed, more or less of the discharge current at the target surface can be carried by the electrons rather than the ions [13, 15]. This means that the current rises for some materials but decreases for others when sputtering in compound (transition) mode.

It has recently been observed that the discharge current waveform in the reactive $Ar/N_2$ [16] and $Ar/O_2$ [17] discharges when sputtering a Ti target, and $Ar/O_2$ discharge when sputtering a Nb target [11], is highly dependent on the pulse repetition frequency. This is significantly different from what is observed for the non-reactive Ar discharge where the discharge current waveform is independent of the repetition frequency [16]. The current is found to increase significantly as the repetition frequency is lowered. This has been attributed to an increase in the secondary electron emission yield for self-sputtering when the nitride or oxide forms on the target at low frequencies [16, 17]. The secondary electron emission yield is higher for a nitrided or oxidized (poisoned) Ti target than a clean Ti target when self-sputtering is the dominant sputtering mechanism, since the electron emission yield for self-sputtering by singly ionized metal is essentially zero, which is not the case for $N^+$ or $O^+$ bombarding the target. This differentiates HiPIMS from dcMS where self-sputtering is not as important.

## 2. Experimental apparatus and method

The experiment was performed in a custom built cylindrical magnetron sputtering chamber, 29 cm in diameter and 25 cm long [18] with a base pressure of

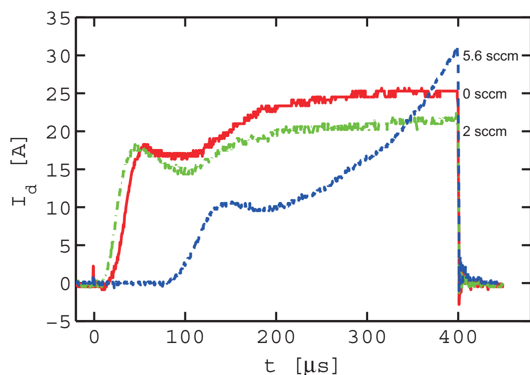


FIG. 1. The discharge current for various oxygen flow rates for $Ar/O_2$ discharge with titanium target. The discharge pressure is roughly 0.6 Pa, the repetition frequency 50 Hz, and the pulse voltage is 600 V.

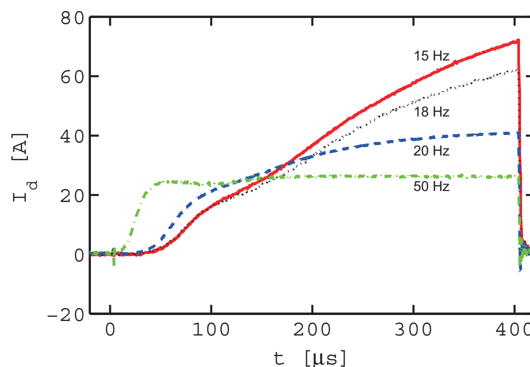


FIG. 2. The discharge current for various repetition frequencies for $Ar/O_2$ discharge with titanium target. The discharge pressure is roughly 0.6 Pa, the oxygen flow rate 2 sccm, and the pulse voltage is 600 V.

$4 \times 10^{-6}$ Pa. The sputtering gas was argon of 99.999% purity mixed with oxygen gas of 99.999% purity. The argon flow rate was $q_{\mathrm{Ar}} = 40$ sccm and the oxygen flow rate was varied resulting in a total pressure of $0.6 \pm 0.1$ Pa. A circular, balanced, planar magnetron was used, fitted with a Ti target, 75 mm in diameter and of 99.995% purity. The power was supplied by a SPIK1000A pulse unit (Melec GmbH) operating in the unipolar negative mode at constant voltage, which in turn was charged by a dc power supply (ADL GS30). The discharge current and voltage was monitored using a combined current transformer and voltage divider unit (Melec GmbH) and the data were recorded with a digital storage oscilloscope (Agilent 54624A). The pulse repetition frequency was varied and the pulse length was 400 $\mu$s.

## 3. Results and Discussion

Figure 1 shows the current waveforms for an $Ar/O_2$ discharge with a Ti target where the oxygen flow rate is varied. The discharge pressure is roughly 0.6 Pa and the pulse voltage is 600 V and this voltage is maintained throughout the pulse. We see that the discharge current decreases when 2 sccm of oxygen is added to the discharge. However, if the oxygen flow is increased to 5.6 sccm a transition is observed. The delay in the onset of the current increases significantly, the initial current peak is significantly lowered and then a transition to a self-sputtering runaway regime occurs. A transition in the $I_{\mathrm{d}} - V_{\mathrm{d}}$ characteristics of a discharge with increasing reactive gas flow is generally interpreted as a transition from metal to compound (oxide) mode. Figure 2 shows how the discharge current waveform varies with repetition frequency. As the repetition frequency is lowered from 50 Hz to 20 Hz we see an increase in the current which transits into a different waveform as we decrease the repetition frequency further. The waveform observed at low repetition frequency is similar to the one observed at high reactive gas flow rate seen in figure 1. This indicates that oxidation takes place between the pulses. As we increase the time between pulses there is more time available for target poisoning.

When an argon discharge is diluted by molecular gas several issues need to be taken into account. When a reactive molecular gas is added to the discharge the collisional energy loss per electron-ion pair created changes. For molecular gases the collisional energy loss per electron-ion pair created can be expected to be a few times higher than for a noble gas due to additional collisional energy losses such as rotational and vibrational excitation. Thus we expect the plasma density to decrease and a slight decrease in the discharge current is expected for a fixed voltage. Furthermore, for molecular ions the secondary electron emission yield is somewhat smaller (for the same ionization energy) due to resonant electron capture [13, 19], which also leads to a decrease in the discharge current. We see this change in figure 1 when we add 2 sccm of $O_2$ to the discharge.

However, HiPIMS differs from dcMS in the important respect that self-sputtering quickly becomes the dominant sputtering mechanism. During the self-sputtering phase the working gas ions (mostly $Ar^+$ and $O_2^+$ or $N_2^+$) are depleted from the area in front of the target (at least to a large extent), so the majority of ions taking part in the sputtering are due to the atoms being supplied by the target that have experienced electron impact ionization. As the secondary electron emission yield is not only dependent on the target composition but also on the ion species bombarding it, this results in a crucial distinction between the two sputtering methods. During the self-sputtering phase of a metal mode discharge, metal ions are bombarding a metallic target. It is known that the secondary electron emission

yield is practically zero in this case, unless multiply charged ions are involved as the electron emission from a metal is only possible when the ionization energy of the bombarding ion exceeds twice the work function of the metal $\phi$ [20]. On the other hand, for a discharge operating in the poisoned mode, self-sputtering will involve both metal ions and ions of the reactive gas ($O^+$ or $N^+$-ions), as such ions are also being supplied by the target via electron impact ionization in this instance. Indeed, it has been confirmed that in the oxide mode, the discharge is dominated by the $O^+$-ion, which is due to oxygen atoms sputtered off the target surface [21]. As the first ionization energy of O or N atoms is large compared to metal atoms the potential emission of secondary electrons will be much larger during the self-sputtering phase when the target is poisoned and hence the large increase in current during the latter part of the pulse is observed.

## 4. Summary

It can be concluded that the behavior of the reactive HiPIMS discharge differs significantly from the non-reactive discharge in a somewhat counterintuitive fashion. The current-voltage-time waveforms in a reactive discharge exhibit similar general characteristics as the non-reactive case in that the current rises to a peak due to gas compression, then decays because of rarefaction before rising to a self-sputtering dominated phase. However, self-sputtering runaway occurs at lower discharge voltages in the reactive discharge due to the formation of oxide or nitride on the target. The secondary electron emission yield is higher for an oxidized or nitrided target than a titanium target when self-sputtering is the dominant sputtering mechanism. This differentiates HiPIMS from dcMS where self-sputtering is not as important. The current rises sharply as the pulse repetition frequency is lowered as a result of increased target oxidation or nitridation. Measurements show that these increases in the self-sputtering phase result in a similar increase in the ion flux impinging on the substrate [16].

**ACKNOWLEDGMENTS**

This work was partially supported by the Icelandic Research Fund Grant No. 130029-051. and the University of Iceland Research Fund. The authors acknowledge useful discussions within COST action MP0804.

[1] U. Helmersson, M. Lattemann, J. Bohlmark, A. P. Ehiasarian, and J. T. Gudmundsson, Thin Solid Films **513**(1-2), 1 (2006).
[2] J. T. Gudmundsson, N. Brenning, D. Lundin, and U. Helmersson, Journal of Vacuum Science and Technology A **30**(3), 030801 (2012).
[3] J. T. Gudmundsson, J. Alami, and U. Helmersson, Surface and Coatings Technology **161**(2-3), 249 (2002).
[4] J. Bohlmark, J. Alami, C. Christou, A. P. Ehiasarian, and U. Helmersson, Journal of Vacuum Science and Technology A **23**(1), 18 (2005).
[5] S. Konstantinidis and R. Snyders, The European Physical Journal – Applied Physics **56**(2), 24002 (2011).
[6] S. Konstantinidis, J. Dauchot, and M. Hecq, Thin Solid Films **515**(3), 1182 (2006).
[7] K. Sarakinos, J. Alami, and M. Wuttig, Journal of Physics D: Applied Physics **40**(7), 2108 (2007).
[8] F. Magnus, A. S. Ingason, O. B. Sveinsson, S. Olafsson, and J. T. Gudmundsson, Thin Solid Films **520**(5), 1621 (2011).
[9] F. Magnus, A. S. Ingason, S. Olafsson, and J. T. Gudmundsson, IEEE Electron Device Letters **33**(7), 1045 (2012).
[10] F. Ruske, A. Pflug, V. Sittinger, W. Werner, B. Szyszka, and D. J. Christie, Thin Solid Films **516**(14), 4472 (2008).
[11] M. Hála, J. Čapek, O. Zabeida, J. E. Klemberg-Sapieha, and L. Martinu, Journal of Physics D: Applied Physics **45**(5), 055204 (2012).
[12] K. Sarakinos, D. Music, S. Mráz, M. to Baben, K. Jiang, F. Nahif, A. Braun, C. Zilkens, S. Konstantinidis, F. Renaux, D. Cossement, F. Munnik, *et al.*, Journal of Applied Physics **108**(1), 014904 (2010).
[13] D. Depla, S. Mahieu, and R. De Gryse, Thin Solid Films **517**(9), 2825 (2009).
[14] S. Berg and T. Nyberg, Thin Solid Films **476**(2), 215 (2005).
[15] D. Depla, S. Heirwegh, S. Mahieu, J. Haemers, and R. De Gryse, Journal of Applied Physics **101**(1), 013301 (2007).
[16] F. Magnus, O. B. Sveinsson, S. Olafsson, and J. T. Gudmundsson, Journal of Applied Physics **110**(8), 083306 (2011).
[17] F. Magnus, T. K. Tryggvason, S. Olafsson, and J. T. Gudmundsson, Journal of Vacuum Science and Technology A **30**(5), 050601 (2012).
[18] U. B. Arnalds, J. S. Agustsson, A. S. Ingason, A. K. Eriksson, K. B. Gylfason, J. T. Gudmundsson, and S. Olafsson, Review of Scientific Instruments **78**(10), 103901 (2007).
[19] R. A. Baragiola, Nuclear Instruments and Methods in Physics Research Section B: Beam Interactions with Materials and Atoms **88**(1-2), 35 (1994).
[20] A. Anders, Applied Physics Letters **92**(20), 201501 (2008).
[21] M. Aiempanakit, A. Aijaz, D. Lundin, U. Helmersson, and T. Kubart, Journal of Applied Physics **113**(13), 133302 (2013).